

Generation of a New Three Dimension Autonomous Chaotic Attractor and its Four Wing Type

Fei Yu

College of Information Science and Engineering
Hunan University
Changsha, China
yufeiyf@yahoo.com.cn

Chunhua Wang

College of Information Science and Engineering
Hunan University
Changsha, China
wch1227164@sina.com

Abstract— In this paper, a new three-dimension (3D) autonomous chaotic system with a nonlinear term in the form of a hyperbolic sine (or cosine) function is reported. Some interesting and complex attractors are obtained. Basic dynamical properties of the new chaotic system are demonstrated in terms of Lyapunov exponents, Poincare mapping, fractal dimension and continuous spectrum. Meanwhile, for further enhancing the complexity of the topological structure of the new chaotic attractors, the attractors are changed from two-wing to four-wing through making axis doubly polarized, theoretically analyzed and numerically simulated. The obtained results clearly show that the chaotic system deserves further detailed investigation.

Keywords- 3D chaotic attractor; chaotic system; hyperbolic sine; four-wing; axis doubly polarized

I. INTRODUCTION

Nonlinear analysis especially chaos analysis and applications in dynamical systems has been studied extensively within many fields, such as secure communication, synchronization and control [1-3]. Since Lorenz found the first chaotic attractor in a simple mathematical model of a weather system which was constituted of three-order ordinary differential equations in 1963 [4], in-depth researches to propose new chaotic attractors have been undergone in the last four decades. In 1976, Rossler conducted important work that rekindled the interest in three-dimensional (3D) dissipative dynamical systems [5]. Then, many Lorenz-like or Lorenz-based chaotic systems were proposed and investigated [6-17].

Creating a chaotic system with a more complicated topological structure such as a multi-wing attractor becomes a desirable task and sometimes a key issue for many engineering applications. Recently, some new four-wing chaotic systems were proposed. Wang et al. discussed the methods to generate a four wing chaotic attractor in detail and gave some sufficient conditions, such as: (1) there is at least one quadratic term in every equation; (2) there are at least three independent variables, and there is at least one linear term in every equation of the system; (3) there are five equilibria [10]. The authors pointed out the quadratic terms are very important in creating a four-wing chaotic attractor [10]. In 2010, Jia et al. reported a four-wing chaotic attractor and the chaotic characteristic of the

system was proved by investigating the existence of a topological horseshoe in it, based on the topological horseshoe theory [11]. In 2011, Wang et al. investigated a four-wing chaotic attractor and demonstrated that there existed heteroclinic orbits [12]. The four-wing chaotic attractors in [11, 12] all meet the four-wing standards proposed in [10].

In this paper, a novel approach to construct a four-wing chaotic attractor is proposed. Firstly a new chaotic attractor is established. It is a 3D autonomous system which mainly relies on a quadratic hyperbolic sine (or cosine) nonlinear term and a quadratic cross-product term to introduce the nonlinearity necessary for folding trajectories, which can generate an attractor through theoretical analysis and detailed numerical simulation. Nonlinear dynamic properties of this system are studied by means of nonlinear dynamics theory, numerical simulation, Lyapunov exponents, Poincare mapping, fractal dimension and continuous spectrum. The compound structure of the two-wing attractor obtained by merging together two simple attractors after performing one mirror operation is explored. Finally, a four-wing type of the new chaotic attractor is realized by using z -axis doubly polarized.

II. NEW 3D AUTONOMOUS CHAOTIC SYSTEM

A new 3D autonomous chaotic system with a non-linear term in the form of a hyperbolic sine (or cosine) function is expressed as follows respectively:

$$\begin{cases} \dot{x} = a(y-x), \\ \dot{y} = bx - cxz, \\ \dot{z} = \sinh(xy) - dz, \end{cases} \quad (1)$$

and

$$\begin{cases} \dot{x} = a(y-x), \\ \dot{y} = bx - cxz, \\ \dot{z} = \cosh(xy) - dz, \end{cases} \quad (2)$$

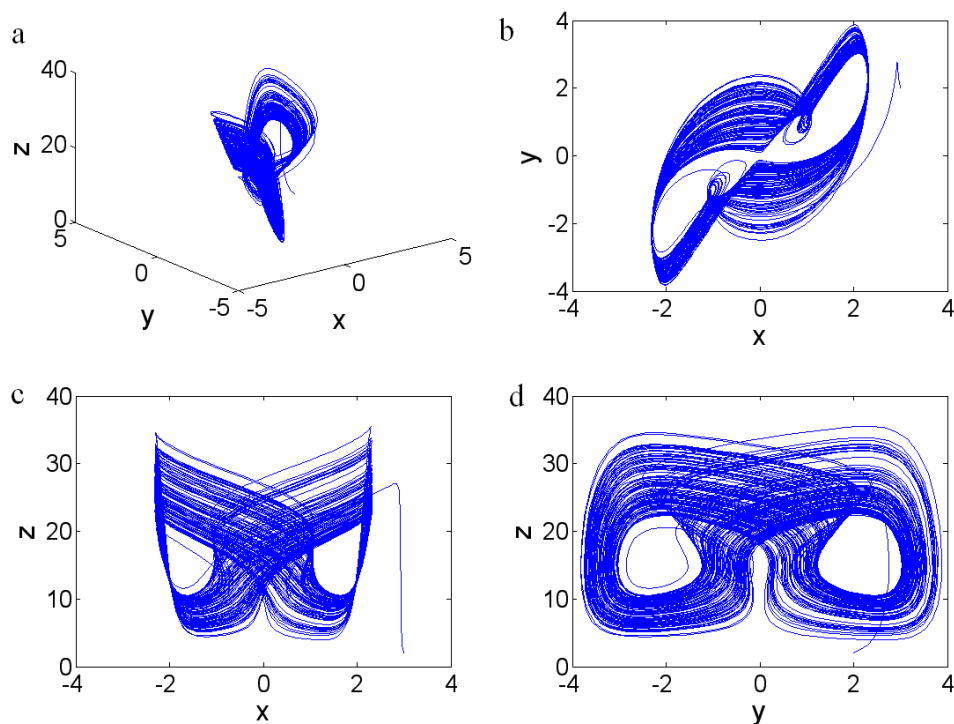


Fig. 1. Phase portraits of system (1) at the initial conditions $[3, 2, 2]^T$. (a) $x-y-z$ view, (b) $x-y$ plane, (c) $x-z$ plane, (d) $y-z$ plane.

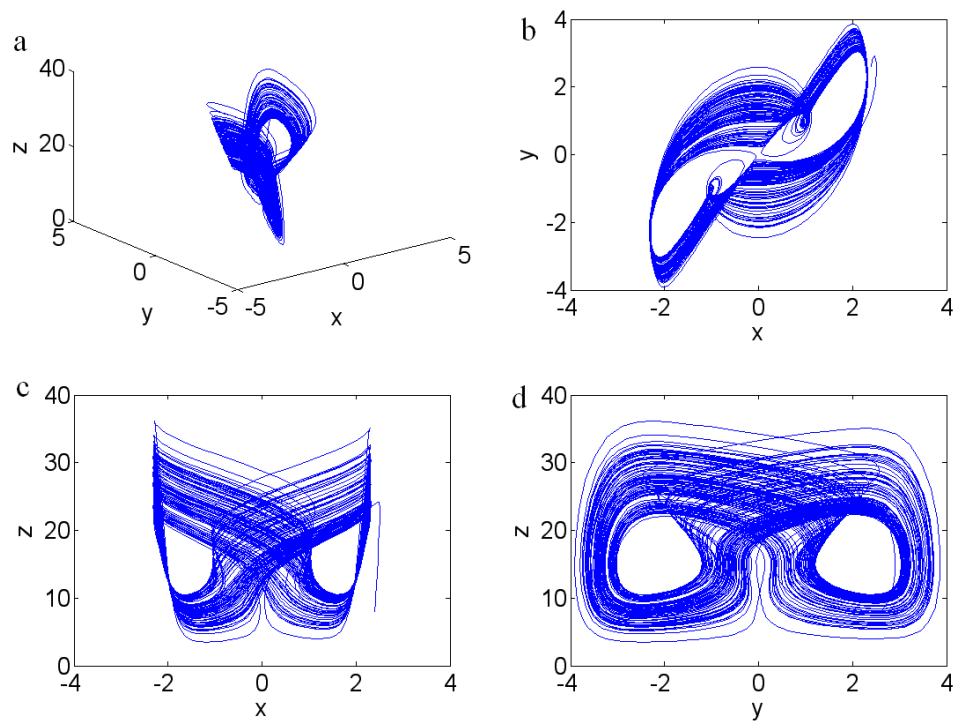


Fig. 2. Phase portraits of system (2) at the initial conditions $[3, 2, 2]^T$. (a) $x-y-z$ view, (b) $x-y$ plane, (c) $x-z$ plane, (d) $y-z$ plane.

where a, b, c, d are real parameters assuming that $a, b, c, d > 0$ and x, y, z are the state variables. Systems (1) and (2) can generate a new two-wing chaotic attractor for the parameters $a = 10, b = 30, c = 2$ and $d = 2.5$. The chaotic attractors are displayed in Figures 1 and 2. It appears that the new attractor exhibits an interesting complex chaotic dynamics behavior.

From Figures 1 and 2, it can be seen that the nonlinear dynamic behaviors for systems (1) and (2) are very similar. So, below we mainly investigate the properties of system (1) since similar methods can be used for research on system (2).

III. BASIC PROPERTIES OF SYSTEM (1)

A. Equilibria

Let:

$$\begin{cases} a(y-x) = 0, \\ bx - cz = 0, \\ \sinh(xy) - dz = 0, \end{cases} \quad (3)$$

If $db > c > 0$, the system has two equilibria points, which are respectively described as follows:

$$E^+ (\sqrt{\ln m}, \sqrt{\ln m}, b/c), E^- (-\sqrt{\ln m}, -\sqrt{\ln m}, b/c).$$

where $m = p + \sqrt{p^2 + 4}/2, p = 2db/c$. When $a = 10, b = 30, c = 2, d = 2.5$, we operate above those nonlinear algebraic equations and obtain that:

$$E^+ (2.0779, 2.0799, 15), E^- (-2.0779, -2.0799, 15).$$

For equilibrium point E^+ , system (1) are linearized, the Jacobian matrix is defined as:

$$J^+ = \begin{pmatrix} -a & a & 0 \\ b - cz & 0 & -cx \\ y \cosh(xy) & x \cosh(xy) & -d \end{pmatrix} = \begin{pmatrix} -10 & 10 & 0 \\ 0 & 0 & -4.16 \\ 77.95 & 77.95 & -2.5 \end{pmatrix}.$$

To gain its eigenvalues, we let $|\lambda I - J^+| = 0$.

These eigenvalues corresponding to the equilibrium point E^+ are $\lambda_1 = -15.9997, \lambda_2 = 1.7498 + 20.0468i$ and $\lambda_3 = 1.7498 - 20.0468i$.

Here λ_1 is a negative real number and λ_2 and λ_3 become a pair of complex conjugate eigenvalues with positive real parts.

The equilibrium point E^+ is a saddle-focus point, and system (1) is unstable at this equilibrium point.

For the equilibrium point E^- , its Jacobian matrix equals to:

$$J^- = \begin{pmatrix} -a & a & 0 \\ b - cz & 0 & -cx \\ y \cosh(xy) & x \cosh(xy) & -d \end{pmatrix} = \begin{pmatrix} -10 & 10 & 0 \\ 0 & 0 & -4.16 \\ 77.95 & 77.95 & -2.5 \end{pmatrix}.$$

The same we let $|\lambda I - J^-| = 0$. These eigenvalues corresponding to the equilibrium point E^- are $\lambda_1 = -15.9997, \lambda_2 = 1.7498 + 20.0468i$ and $\lambda_3 = 1.7498 - 20.0468i$.

Apparently λ_1 is a negative real number and λ_2 and λ_3 form a complex conjugate pair and their real parts are positive. The equilibrium point E^- is also a saddle-focus point, and system (1) is unstable at this equilibrium point.

By the above brief analysis, the two equilibrium points of the non-linear system are all saddle focus-nodes.

B. Symmetry and invariance

It is easy to see the invariance of system under the coordinate transformation $(x, y, z) \rightarrow (-x, -y, z)$, i.e., the system has rotation symmetry around the z-axis [16]. The orbit on the z-axis tends to the origin as $t \rightarrow \infty$.

C. Dissipativity and the existence of attractor

The three Lyapunov exponents and the divergence of the vector field is:

$$\sum_{i=1}^3 LE_i = \Delta V = \frac{\partial \dot{x}}{\partial x} + \frac{\partial \dot{y}}{\partial y} + \frac{\partial \dot{z}}{\partial z} = -(a+d) = f, \quad (4)$$

where $LE_i (i=1, 2, 3)$ denote the three Lyapunov exponents of the system. Note that $f = -(a+d) = -12.5$ is a negative value, so the system is a dissipative system and an exponential rate is:

$$\frac{dV}{dt} = e^f = e^{-12.5}. \quad (5)$$

From (5), it can be seen that a volume element V_0 is contracted by the flow into a volume element $V_0 e^{-12.5t}$ in time t . This means that each volume containing the system trajectory shrinks to zero as $t \rightarrow \infty$ at an exponential rate of -12.5 . Therefore, all system orbits are ultimately confined to a specific subset having zero volume and the asymptotic motion settles onto an attractor [14, 15, 17].

D. Lyapunov exponent and fractional dimension

The Lyapunov exponents refer to the average exponential rates of divergence or convergence of nearby trajectories in the phase space [13, 17]. If there is at least one positive Lyapunov exponent, the system can be defined to be chaotic. The Lyapunov exponents are calculated to be $l_1 = 0.6649$, $l_2 = 0$ and $l_3 = -13.1763$. Therefore, the Lyapunov dimension of this system is:

$$D_L = j + \frac{\sum_{i=1}^j l_i}{|l_{j+1}|} = 2 + \frac{l_1 + l_2}{|l_3|} = 2 + \frac{0.6776}{|-13.1763|} = 2.0514 \quad (6)$$

Equation (6) means system (1) is really a dissipative system, and the Lyapunov dimensions of the system are fractional. Having a strange attractor and positive Lyapunov exponent, it is obvious that the system is really a 3D chaotic system.

E. Time domain, spectrum map and Poincare maps

In the time domain, Figure 3 shows an apparently chaotic waveform $x(t)$ of system (1) whilst, in the frequency domain, an apparently continuous broadband spectrum $\log|x|$ of system (1) is shown in Figure 4. It can be seen from Figures 3 and 4 that the new system exhibits chaotic behaviors. The Poincare maps are shown in Figure 5. From Figures 5(a) and 5(b), it can be seen that the Poincare maps consist of virtually symmetrical branches. We can further find that the section of the attractor looks like the tangled points from the Poincare map of system (1) as shown in Figures 5(c) and 5(d).

F. Lyapunov exponent spectrum

Figure 6 shows the Lyapunov exponent spectrum versus increasing c . It can be observed that the system is undergoing some representative dynamical routes, such as stable fixed points, chaos and period-doubling bifurcation. For example, when the parameters $a = 10$, $b = 30$, $d = 2.5$, while c is varied on the closed interval $(0, 20]$, we can summarize as follows:

- $0 < c \leq 1.04$, $l_1 = 0$, $l_2 \leq 0$, $l_3 < 0$, there is a reverse period-doubling bifurcation route with a flip bifurcation, the system are some period-doubling bifurcation windows, one is shown in Figure 7(a)
- $1.04 < c \leq 6.66$, $l_1 > 0$, $l_2 = 0$, $l_3 < 0$, the system is chaotic as shown in Figure 7(b), and there are several periodic windows in the chaotic band.
- $6.66 < c \leq 9.11$, $l_1 = 0$, $l_2 \leq 0$, $l_3 < 0$, the system are some period-doubling bifurcation windows, one is shown in Figure 7(c).
- $9.11 < c \leq 20$, $l_1 > 0$, $l_2 = 0$, $l_3 < 0$, the system is chaotic as shown in Figure 7(d), and there are several periodic windows in the chaotic band.

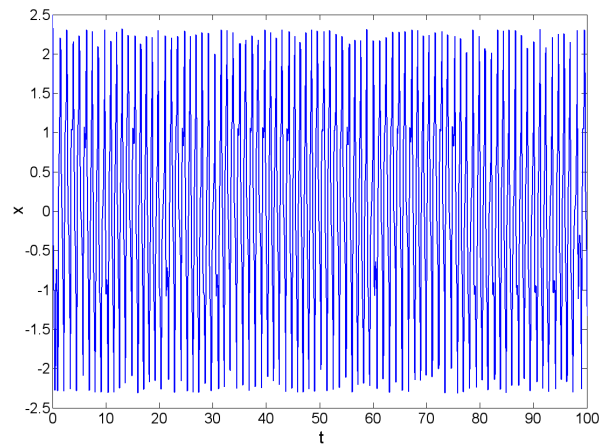


Fig. 3. Chaotic waveform of $x(t)$.

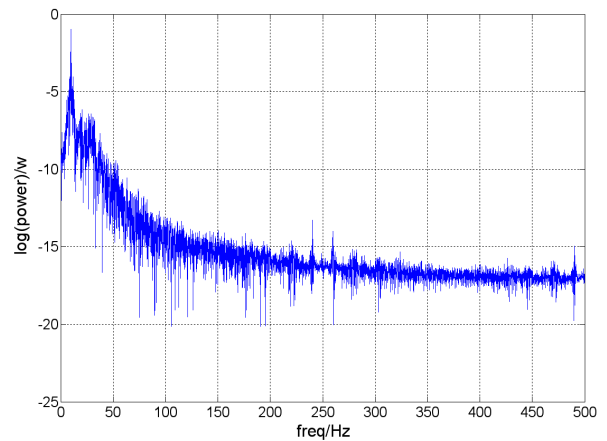


Fig. 4. Continuous broadband frequency spectrum of $\log|x|$.

G. Forming mechanism of this new chaotic attractor structure

Compound structures of system (1) may be obtained by merging together two simple attractor after performing one mirror operation [8, 17]. Such an operation can be revealed through the use of a controlled system of the form:

$$\begin{cases} \dot{x} = a(y - x) \\ \dot{y} = bx - cxz + u \\ \dot{z} = \sinh(xy) - dz \end{cases} \quad (7)$$

where u is a parameter of control and the value of u can be changed within a certain range. Here, we still select the initial values of the system as $[3, 2, 2]^T$. When $u = 0.1$, the attractor evolves into partial but is still bounded in this time, the corresponding strange attractors are shown in Figure 8(a). When $u = 4.2$, the attractors are evolved into the single right

scroll attractor, it is only one half the original chaotic attractors in this time, the corresponding strange attractors are shown in Figure 8(b). Then we set u to be a negative value. When $u = -0.1$, the corresponding strange attractors are shown in Figure 8(c), the attractor evolves into partial but is still

bounded in this time. When $u = -4.2$, the corresponding strange attractors are shown in Figure 8(d), the attractors are evolved into the single left scroll attractor; it is only one half the original chaotic attractors in this time.

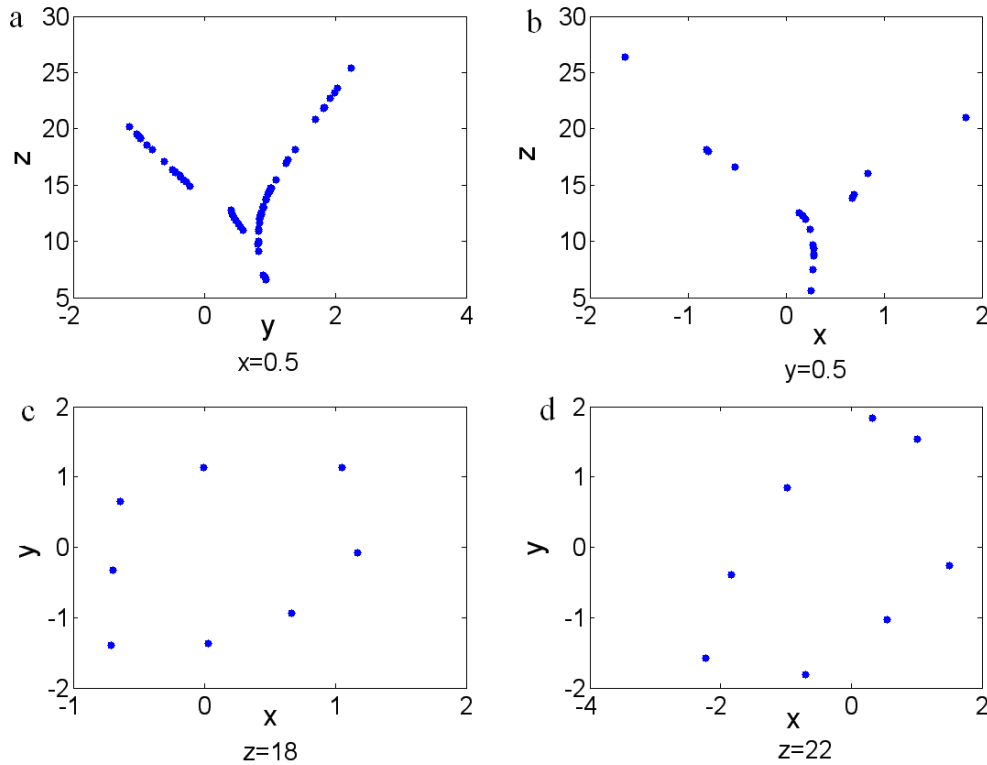


Fig. 5. Poincaré maps in planes where (a) $x = 0.5$, (b) $y = 0.5$, (c) $z = 18$, (d) $z = 22$.

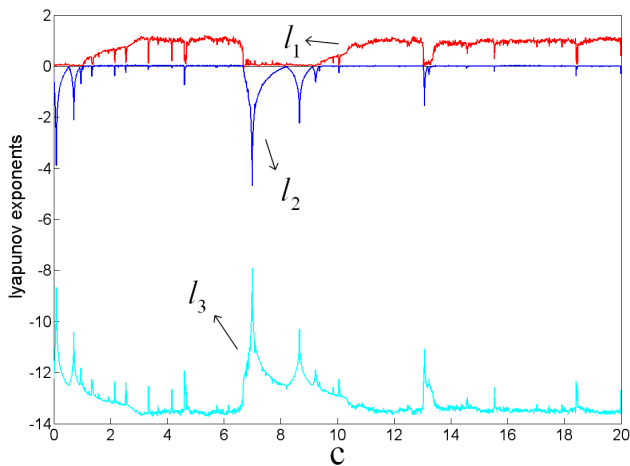


Fig. 6. Lyapunov exponents spectrum of system (1) with $c \in (0, 20]$

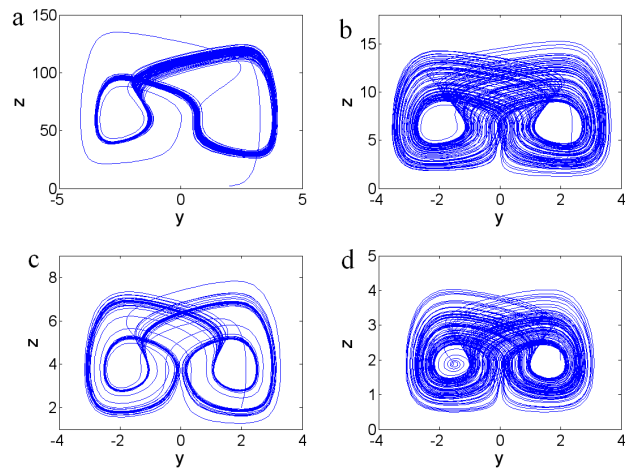


Fig. 7. Phase portraits of system (1) with $(a,b,d) = (10,30,2.5)$ at initial values $[3,2,2]^T$, (a) $c = 0.5$, (b) $c = 4.7$, (c) $c = 8$, (d) $c = 16$.

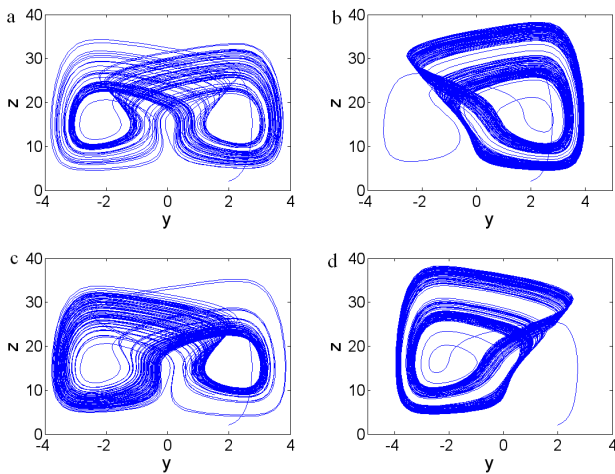


Fig. 8. Phase portraits of system (6) in $y-z$ plane at (a) $u = 0.1$, (b) $u = 4.2$, (c) $u = -0.1$, (d) $u = -4.2$.

IV. A FOUR-WING TYPE OF SYSTEM (1)

A four-wing type of system (1) is studied in this section. First, we simply introduce the anti-structure of system (1). Then, two architectures are unified by one system. In order to connect with the up-tractor and down-tractor, we use z -axis doubly polarized, and the attractors of system (1) will be changed from two-wing to four-wing. The principle will be discussed in detail below.

A. Anti-structure of system (1)

The anti-structure of system (1) can be expressed as:

$$\begin{cases} \dot{x} = a(y-x) \\ \dot{y} = bx + cz \\ \dot{z} = -\sinh(xy) - dz \end{cases} \quad (8)$$

Under the same parameters conditions, system (8) is also chaotic. The chaotic attractor is displayed in Figure 9(b). It appears that the new attractor locates in the quadrant of $z < 0$, while the attractor of system (1) is in the quadrant of $z > 0$ (Figure 9(a)).

B. Uniform structure of system (1) and system (8)

By using sign function, the uniform structure of system (1) and system (8) can be expressed as:

$$\begin{cases} \dot{x} = a(y-x) \\ \dot{y} = bx - cz \cdot \text{sign}(z) \\ \dot{z} = \text{sign}(z) \cdot (\sinh(xy) - dz \cdot \text{sign}(z)) \end{cases} \quad (9)$$

Under the same parameters conditions, system (9) is also chaotic. The chaotic attractor is displayed in Figure 9(c). The full line is the trajectory of system (1) and the dotted line is the trajectory of system (8). It can be seen that the chaotic attractors can not evolve from negative half shaft to positive half shaft, and vice versa. So there are unable to produce a four-wing chaotic attractor.

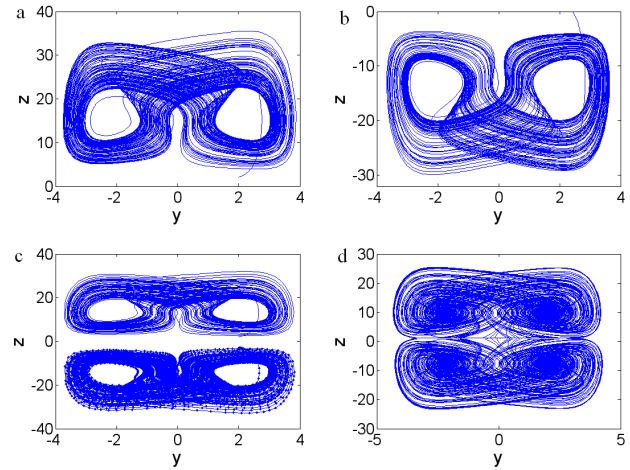


Fig. 9. Phase portraits of (a) system (1), (b) system (8), (c) system (9), (d) system (10) in $y-z$ plane.

C. A new four-wing chaotic attractor

In order to connect with up-tractor and down-tractor, we do coordinate translation along the z -axis to zero point of system (9). Then, we get a four-wing system which can be expressed as:

$$\begin{cases} \dot{x} = a(y-x) \\ \dot{y} = bx - cz \cdot (z \cdot \text{sign}(z) + 10) \\ \dot{z} = H(z) \cdot (\sinh(xy) - d \cdot (z \cdot \text{sign}(z) + 10)) \end{cases} \quad (10)$$

where $H(z)$ is the hysteretic function, and the expression can be expressed as

$$H(z) = \begin{cases} 1, & z \rightarrow 1 \\ -1, & z \rightarrow -1 \end{cases} \quad (11)$$

The four-wing chaotic attractor is displayed in Figure 9(d). From Figure 9(d), it can be seen that the four-wing chaotic attractor is symmetrical around the $x-y$ plane. With further research, when the parameters $a = 4.4$, $b = 46$, $d = 2.6$, while c is varied, the four-wing chaotic attractor of system (10) can exhibit very interesting dynamics behavior. The system is undergoing some novel dynamical routes, such as down-period-down-chaos (Figure 10(c)), up-period-doubling-down-

chaos (Figure 10(d)), up-period-doubling-down-period-doubling (Figure 10(e)) and down-sink (Figure 10(f)), it notes that here up means the area of $z > 0$, down means the area of $z < 0$. Using the same mathematical methods as presented in

section 3 for analyzing system (10), system (10) also has some basic dynamical properties, such as equilibria, symmetry, invariance, dissipativity, fractional dimension and so on.

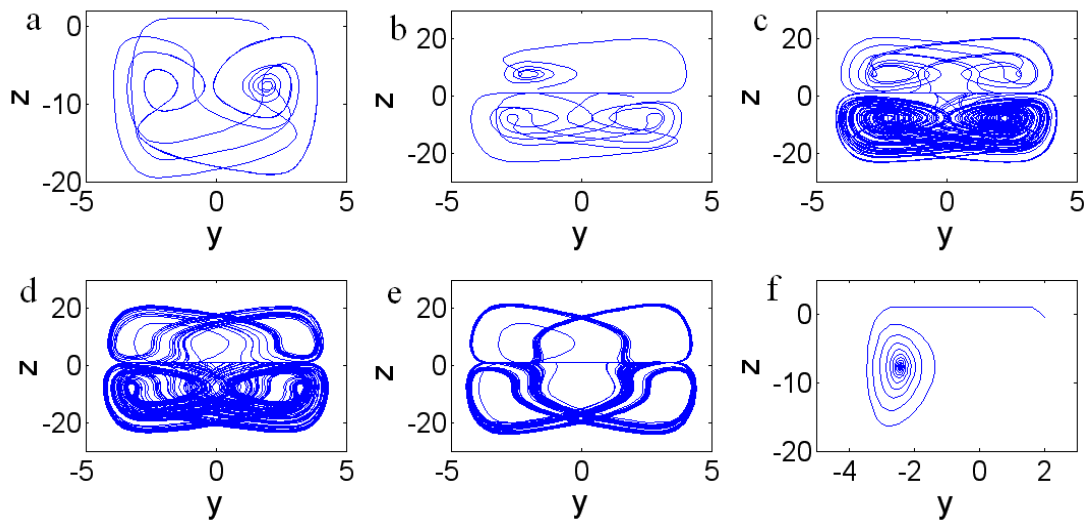


Fig. 10. Phase portraits of system (10) in $y-z$ plane at (a) $c=1.2$, (b) $c=1.58$, (c) $c=1.9$, (d) $c=2.7$, (e) $c=3.8$, (f) $c=10$.

V. CONCLUSION

A new 3D autonomous chaotic system with a nonlinear term in the form of a hyperbolic sine (or cosine) function is presented. The dynamical behaviors of the new system are analyzed, both theoretically and numerically, including some basic dynamical properties, Lyapunov exponents, Poincare mapping, routes to chaos and so on. In addition, forming mechanisms of compound structures of the new chaotic attractor have been studied and explored. Further, a new four-wing chaotic attractor is realized by using doubly polarized z -axis, more suitable for secure communication applications due to the complexity of its topological structure.

REFERENCES

- [1] A. A. Zaher, A. Abu-Rezq, "On the design of chaos-based secure communication systems", *Commun. Nonlinear Sci. Numer. Simulat.*, Vol. 16, No. 9, pp. 3721-3737, 2011
- [2] X. Wang, J. Song, "Synchronization of the unified chaotic system", *Nonlinear Analysis: Theory, Methods & Applications*, Vol. 69, No. 10, pp. 3409-3416, 2008
- [3] C. Zhu, "Feedback control methods for stabilizing unstable equilibrium points in a new chaotic system", *Nonlinear Analysis: Theory, Methods & Applications*, Vol. 71, No. 7-8, pp. 2441-2446, 2009
- [4] E. N. Lorenz, "Deterministic non-periodic flow", *J. Atmos. Sci.*, Vol. 20, No. 1, pp. 130-141, 1963
- [5] O. E. Rossler, "An equation for continuous chaos", *Phys. Lett. A*, Vol. 57, No. 5, pp. 397-398, 1976
- [6] G. Chen, T. Ueta, "Yet another chaotic attractor", *Internat. J. Bifur. Chaos*, Vol. 9, No. 7, pp. 1465-1457, 1999
- [7] J. Lü, G. Chen, "A new chaotic attractor coined", *Internat. J. Bifur. Chaos*, Vol. 12, No. 3, pp. 659-661, 2002
- [8] C. Liu, T. Liu, L. Liu, K. Liu, "A new chaotic attractor", *Chaos, Solitons Fractals*, Vol. 22, No. 5, pp. 1031-1038, 2004
- [9] S. Celikovsky, G. Chen, "On the generalized Lorenz canonical form", *Chaos, Solitons Fractals*, Vol. 26, No. 5, pp. 1271-1276, 2005
- [10] Z. Wang, G. Qi, Y. Sun, B. J. van Wyk, M. A. van Wyk, "A new type of four-wing chaotic attractors in 3-D quadratic autonomous systems", *Nonlinear Dyn.*, Vol. 60, No. 3, pp. 443-457, 2010
- [11] H. Jia, Z. Chen, G. Qi, "Topological horseshoe analysis and the circuit implementation for a four-wing chaotic attractor", *Nonlinear Dyn.*, Vol. 65, No. 1-2, pp. 131-140, 2011
- [12] X. Wang, J. Li, J. Fang, "The stability and chaotic motions of a four-wing chaotic attractor", *Appl. Mech. Mater.*, Vol. 48-49, No. 2, pp. 1315-1318, 2011
- [13] Z. Wei, Q. Yang, "Dynamical analysis of a new autonomous 3-D chaotic system only with stable equilibria", *Nonlinear Analysis: Real World Applications*, Vol. 12, No. 1, pp. 106-118, 2011
- [14] X. F. Li, K. E. Chlouvakis, D. L. Xu, "Nonlinear dynamics and circuit realization of a new chaotic flow: A variant of Lorenz, Chen and Lü", *Nonlinear Analysis: Real World Applications*, Vol. 10, No. 4, pp. 2357-2368, 2009
- [15] W. Zhou, Y. Xu, H. Lu, L. Pan, "On dynamics analysis of a new chaotic attractor", *Phys. Lett. A*, Vol. 372, No. 36, pp. 5773-5778, 2008
- [16] S. Dadras, H. R. Momeni, "A novel three-dimensional autonomous chaotic system generating two, three and four-scroll attractors", *Phys. Lett. A*, Vol. 373, No. 40, pp. 3637-3642, 2009
- [17] F. Yu, C. Wang, "A Novel Three Dimension Autonomous Chaotic System with a Quadratic Exponential Nonlinear Term", *Eng. Technol. Appl. Sci. Res.*, Vol. 2, No. 2, pp. 209-215, 2012